

Article

Crystal Structure of a Putative Modulator of Gyrase (TldE) from *Thermococcus kodakarensis*

Xin Zhang ¹, Zhengqun Li ², Yanxiang Zhao ³, Xilan Cheng ¹, Yang Liu ¹, Shihong Zhang ^{2,*} and Junfeng Liu ^{1,*}

¹ Ministry of Agriculture Key Laboratory of Pest Monitoring and Green Management and Joint Laboratory for International Cooperation in Crop Molecular Breeding, College of Plant Protection, China Agricultural University, Beijing 100193, China; zhangxin1506@126.com (X.Z.); chengxilan1026@163.com (X.C.); yangliu_neau@foxmail.com (Y.L.)

² College of Plant Sciences, Jilin University, Changchun 130062, China; lizhengqun1990@163.com

³ College of Plant Health and Medicine, and Key Lab of Integrated Crop Disease and Pest Management of Shandong Province, Qingdao Agricultural University, Qingdao 266000, Shandong, China; hellozyx@yeah.net

* Correspondence: zhang_sh@jlu.edu.cn (S.Z.); jliu@cau.edu.cn (J.L.);
Tel.: +86-431-87835708 (S.Z.); +86-10-62732037 (J.L.)

Received: 15 January 2019; Accepted: 15 February 2019; Published: 19 February 2019



Abstract: TldD and TldE proteins interact and form a complex to degrade unfolded peptides. The gene *Tk0499* from *Thermococcus kodakarensis* encoded a putative modulator of gyrase (*TkTldE*). Although *TldE* genes were common in bacteria and archaea, the structural basis on the evolution of proteins remained largely unknown. Here, the three-dimensional structure of *TkTldE* was determined by X-ray diffraction. Crystals were acquired by the sitting-drop vapor-diffusion method. X-ray diffraction data from crystals were collected at 2.35 Å. The space group and unit-cell parameters suggested that there were two molecules in the asymmetric unit. Our results showed that *TkTldE* forms a homodimer, which contained anti-parallel β-strands and a pair of α-helices. Comparison of the structures of TldE and TldD showed that despite their high sequence similarity, TldE lacked the conserved HExxxH and GxC motif in which two His and a Cys residues bound a metal ion. Taken together, these results provided insight into the structural information of this class of TldE/TldD.

Keywords: TldE; crystal structure; *Thermococcus kodakarensis*

1. Introduction

The *TldD* and *TldE* genes, which encoded a putative protease complex, were common in archaeobacteria and eubacteria [1]. It was reported that TldD/TldE were involved in degrading unfolded peptides by two pathways—i.e., antibiotic peptide microcin B17 (MccB17) production and CcdA antidote degradation—in prokaryotes to ensure the survival of prokaryotic cells [2,3]. MccB17 was secreted by *Escherichia coli* strains containing the plasmid pMccB17 [3]. MccB17 production and immunity required seven genes (*mcbA*, *B*, *C*, *D*, *E*, *F*, and *G*) [4,5]. The *mcbA* gene encoding the MccB17 synthetase synthesized a precursor peptide of 69 amino acids [6]. The products of *McbBCD* genes modified the precursor peptide into an active antibiotic (MccB17), transforming the cysteine and serine residues of the peptide into thiazole and oxazole [7]. The products of the *mcbE* and *mcbF* genes took part in the export of mature MccB17, and that of *mcbG* conferred immunity upon MccB17 [8,9]. MccB17 inhibited DNA gyrase, which was a prokaryotic type-II topoisomerase, leading to the induction of the SOS repair system, double-strand breaks, and ultimately, cell death [10–13]. A chromosomal gene called *pmbA* (or *TldE*) was involved in the cleavage of the MccB17 leader peptide

in the final step and secretion of MccB17 [3]. It has been reported that in *pmbA* (*TldE*) or its homologous *TldD* mutant, pro-MccB17 cannot be released from cells, and so inhibited DNA replication [1,3]. Although the TldD and TldE proteins had high sequence similarity, only TldD contained a conserved metalloprotease-like HExxxH sequence motif that might contribute to catalysis [14]. Ghilarov reported that a heterodimeric TldD/TldE complex was needed for the cleavage of the N-terminal of the modified MccB17 precursor peptide to yield the mature antibiotic [15]. In the CcdA/CcdB poison-antipoison system, CcdA interacted with CcdB to inhibit the cytotoxic activity of CcdB [16]. CcdB inhibited the DNA supercoiling activity of gyrase and was lethal to bacteria [17]. Both TldD and TldE (*pmbA*) were involved in CcdA antidote degradation [1].

Recently, a few studies have focused on archaeal TldD/TldE proteins. TldD/TldE from archaeobacteria were different to those from eubacteria. The structure of a putative modulator of DNA gyrase (TldE) from *Thermotoga maritima* was reported, but shed little light on its functions as a modulator of DNA gyrase [18]. Sso0660 from *Sulfolobus solfataricus*, a TldD homologue, could function alone as a metalloprotease, as it could proteolytically degrade azocasein and FITC-BSA substrates with a zinc ion as its cofactor [14]. The function of these homologous TldD/TldE proteins in *Thermococcus kodakarensis* has not been reported. Whether or not the TldE encoded a metalloprotease remains to be explored in further biological studies.

Here, we cloned a *TldE* gene from the *Thermococcus kodakarensis* genome [19] and reported its crystal structure. Multiple sequence alignment with other organisms TldDs/TldEs and structure comparisons with homologues revealed that they shared a conserved fold with a family of the metalloprotease class. However, detailed comparisons showed that *TkTldE* bore no conserved HExxxH motifs in the vicinity of the corresponding active pocket of *EcTldD*. These results provide a structural basis for further investigation of the function of these proteins.

2. Materials and Methods

2.1. Macromolecule Production

The full-length *TkTldE* consists of 1323 bp encoding 441 amino acid residues. Gene fragments were amplified and inserted into expression vector pHAT2 with NcoI and XhoI, including N-terminal 6xHis, using sticky-end cloning [20] (Table 1). The correctness of the recombinant plasmids was confirmed by sequencing. The prepared TldE construct was transformed into *E. coli* strain BL21(DE3) cells for protein expression. Cells with the recombinant plasmids were grown at 310 K (optical density 0.6–0.8), and expression was induced overnight with 0.4 mM IPTG at 289 K. After harvesting, the cells were resuspended in buffer (20 mM Tris, 150 mM NaCl, pH 7.5) and lysed by sonication. The His-tagged protein in filtered supernatant was obtained by centrifugation and applied to an Ni-NTA agarose column (GE Healthcare) pre-equilibrated with buffer (20 mM Tris, 150 mM NaCl, pH 7.5). The column was washed with four column volumes of lysis buffer containing 20 mM imidazole, and the protein was eluted using 500 mM imidazole. The protein eluate was concentrated in a centrifugal concentrator (Millipore) and applied to a Superdex 200 Increase gel filtration column pre-equilibrated with 20 mM Tris and 150 mM NaCl at pH 7.5 (Table 2). The collected protein was concentrated to 10 mg/mL for crystal screening.

Table 1. Macromolecule production information.

Source Organism	<i>Thermococcus Kodakarensis</i>
Forward primer	F1: CATGGAGAACCTCATACGCTTCGGC F2: GAGAACCTCATACGCTTCGGC
Reverse primer	R1: GTCACCTGCCCGCTATCTTCA R2: TCGAGTCACTTGCCCGCTATCTTCA
Cloning vector	pHAT2
Expression host	<i>E. coli</i> BL21(DE3)

Table 1. Cont.

Source Organism	<i>Thermococcus Kodakarensis</i>
Complete amino-acid sequence of the construct produced	MSHHHHHSMENLIRFGKFFDELEIAVYRS RDIEASVELNEISMASTRSGALTIIRGIKDKRLG LAIVDSDEPEKVKEAIEQAAKMAKLNSPDEK WVSLPEPGKYREKPKPNYELKEASPDILVEKL VKGIKLAREKDKNAVVAGGAGGVSWEERHV LNSHGLDVFQEGGAAYMYLEIVGRKGSVVT GIFDFDARRDLNLDVEGIVERAVQKVQWAY NVVPSKNEEVPLIFGPWAIAGLFSYTLPAFSG ERLVKETTPLAGKVGEKIASEVITLYDDPFHPL SLRPTIADDEGVPTRKNVLIENGAFKGFVWD NYWAKIYGTSTGNGKRDIRSGGINIFHSVVI ENGRSLEDIIGEIDRGYLVLDGLQGAHSSNPD NGNFAVTANPAFLIEDGEVKGSVFLIAGNV YELLQQASEVSKEQTVMPFMNTMITPHIKFEN VKIAGK

Table 2. Crystallization information.

	TIDE
Method	Sitting-drop vapor diffusion
Plate type	96-well plates
Temperature	291 K
Protein concentration (mg/mL)	10
Buffer composition of protein solution	20 mM Tris-HCl, pH 7.5, 150 mM NaCl
Composition of reservoir solution	0.02 M Calcium Chloride, 0.1 M Sodium Acetate pH 4.6, 30% <i>v/v</i> MPD
Volume and ratio of drop	0.5 μ L, 0.25 μ L protein solution: 0.25 μ L reservoir solution
Volume of reservoir (μ L)	35

2.2. Crystallization, Data Collection, and Processing

Initially, crystallization conditions were obtained from commercially-available crystallization screening kits from Hampton Research (Aliso Viejo, CA, USA), and screening was performed at 291 K by the sitting-drop diffusion method with an Oryx4 robot (Douglas Instruments Ltd. Berkshire, UK). Drops consisting of 0.25 μ L protein solution and 0.25 μ L reservoir solution were equilibrated against a 35 μ L reservoir solution. Initial crystals appeared for several conditions of three kits (PEG/ION1, PEG/ION SCREEN, and PEG/ION2 SCREEN). The reservoir solution (0.02 M calcium chloride, 0.1 M sodium acetate, pH 4.6, 30% *v/v* MPD), which gave the best initial crystal morphology, was further optimized by changing the precipitant concentration and introducing additives. The best crystals were obtained after 7 days. Crystallization details are shown in Table 2.

Crystals were soaked in a well solution supplemented with 20% glycerol, and then flash-cooled in liquid nitrogen before data collection. X-ray diffraction data were collected using an ADSC Q315 CCD detector on beamline BL17U1 at the Shanghai Synchrotron Radiation Facility. The data sets were indexed, integrated, and scaled using the HKL-2000 package [21]. Data collection and processing statistics are shown in Table 3.

Table 3. Data collection and processing.

Proteins for Crystallization	TkTIDE
Diffraction source	BL17U1, SSRF
Wavelength (\AA)	0.9791
Temperature (K)	100
Detector	ADSC Q315 CCD
Crystal-detector distance (mm)	300

Table 3. Cont.

Proteins for Crystallization	TkTIDE
Rotation range per image (°)	0.5
Total rotation range (°)	280
Exposure time per image (s)	0.70
Space group	P43212
<i>a</i> , <i>b</i> , <i>c</i> (Å)	104.50 104.50 253.93
α , β , γ (°)	90.00, 90.00, 90.00
Mosaicity (°)	0.30
Resolution range (Å)	30.78–2.35 (2.44–2.35) ^a
Total no. of reflections	659251
No. of unique reflections	59216 (2896)
Completeness (%)	99.90 (100.00)
Redundancy	11.10 (11.60)
$\langle I/\sigma(I) \rangle$	29.67 (2.92)
<i>R</i> _{r.i.m.}	0.05 (0.51)
Overall <i>B</i> factor from Wilson plot (Å ²)	44.15

^a: Numbers in parenthesis are for the highest resolution data shell.

2.3. Structure Solution and Refinement

The structure was solved by molecular replacement using Phaser with 1VL4 as a search model [22], and the model was rebuilt interactively using Coot [23] and phenix.refine until the free R factor converged. The final model was validated using MolProbity [24]. The details of the data collection and refinement statistics are presented in Table 4.

Table 4. Structure refinement.

	TkTIDE
Resolution range (Å)	30.78–2.35 (2.44–2.35) ^a
<i>R</i> _{merge} ^b (%)	16.30 (16.38)
<i>R</i> _{meas} (%)	17.50 (17.44)
CC ^{1/2} (%)	99.60 (71.30)
<i>R</i> _{work} ^c (%)	19.56 (27.46)
<i>R</i> _{free} (%)	22.83 (29.58)
Number of non-hydrogen atoms	7110
macromolecules	6854
Protein residues	884
R.m.s.d.	
Bond lengths (Å)	0.009
Bond angle (°)	1.34
Ramachandran plot (%) ^d	
Ramachandran favored	97.95
Ramachandran allowed	2.05
Ramachandran outliers	0.00
Rotamer outliers	0.69
Clashscore	6.20
Average B-factor	44.82
macromolecules	44.74
solvent	46.89

^a: Numbers in parenthesis are for the highest resolution data shell. ^b: $R_{merge} = \sum_{hkl} \sum_i (|I_i(hkl)| - \langle I(hkl) \rangle) / \sum_{hkl} \sum_i I_i(hkl)$. ^c: $R_{work} = \sum_{hkl} (|F_{obs}| - |F_{calc}|) / \sum_{hkl} |F_{obs}|$. ^d: As evaluated by MolProbity.

3. Results and Discussion

TkTIDE crystals were obtained by the sitting-drop diffusion method and belonged to *P43212*, with unit cell parameters *a* = 104.50 Å, *b* = 104.50 Å, and *c* = 253.93 Å (Figure 1B). The structure was solved by the molecular replacement method using 1VL4 (a putative modulator of a DNA gyrase) as the

initial model. There were two molecules in the asymmetric unit, with a solvent content of 46.89% (Figure 2A). The overall structure of TldE (Protein Data Bank (PDB): 6J6A) was shown in the topology diagram in Figure 2B. TldE subunits formed a hollow core homodimer, which was consistent with the gel filtration results (Figure 1A). The dimer interface consisted of 20 hydrogen bonds and two salt bridges (K77 and D113) (Figure S1). Like other protease family members, one subunit of *TkTldE* contained 11 α -helices and 21 β -strands (Figure 2B). As described for PmbA (PDB: 1VL4) [18] and *E. coli* TldD and TldE (PDB: 5NJ9) [15], one subunit of *TkTldE* contained two domains. The N-terminal domain was composed of six anti-parallel β -strands and five α -helices distributing on the outer surface of β -sheet. The C-terminal domain consisted of a six-stranded anti-parallel β barrel, seven β -strands, and five α -helices, which were strongly twisted (Figure 2).

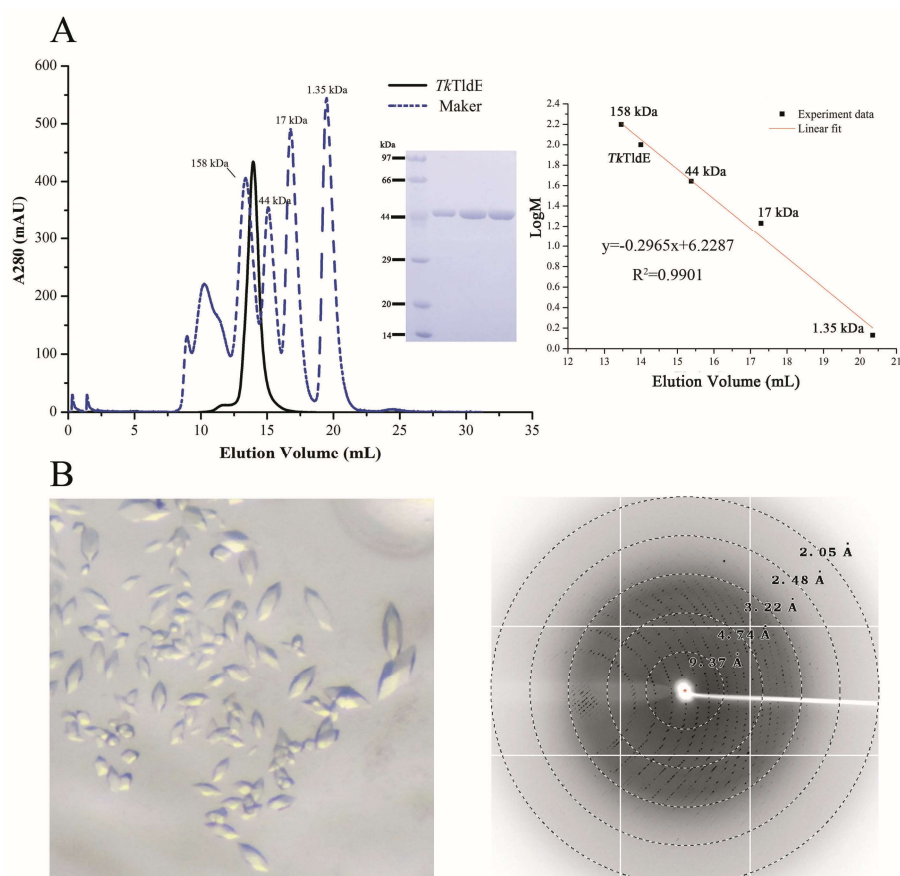


Figure 1. Size-exclusion chromatogram and crystals of *TkTldE*. **(A)** Sodium dodecyl sulfate polyacrylamide gel electrophoresis profile of protein samples after size-exclusion chromatogram. Four experiment data points (13.46 mL/158 kDa, 15.38 mL/44 kDa, 17.29 mL/17kDa, 20.35 mL/1.35 kDa) from the Gel Filtration Standard (Bio-Rad, Cat: 1511901) was used for the column calibration. *TkTldE* was eluted at about 14.18 mL with superdex 200 column and the molecular weight was calculated as approximate 105 kDa in solution. **(B)** Crystal image and the representative X-ray diffraction image of a *TkTldE* crystal. Diffraction resolutions were labelled as circles.

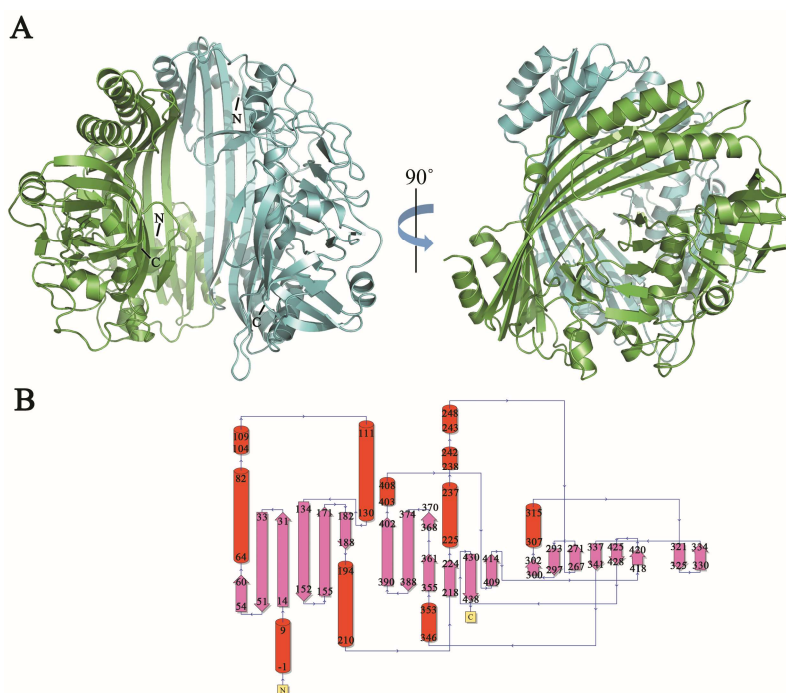


Figure 2. Overall structure of TldE homodimer. **(A)** Two molecules were shown as blue and green cartoons. N- and C-termini were labelled in each molecule. **(B)** Corresponding topology diagrams of the TldE structure. The 21 β -strands were shown as arrows and 11 α -helices as cylinders.

In a structural similarity search, only five structures similar to *TkTldE* deposited in the PDB were found: 5NJ9, 1VL4, 3TV9, 1VPB and 3QTD. All structures except for 5NJ9 formed spherical homodimers without any recognizable catalytic site. The hydrogen bond/salt bridge network contributed to the stability of all dimers. Multiple alignments based on secondary structure of eight representative sequences, TldE from *T. kodakarensis* (*TkTldE*, 6J6A), TldE and TldD from *E. coli* (*EcTldE*/*TldD*, 5NJ9), TldE from *T. maritime* (*TmTldE*, 1VL4), TldE from *Shigella flexneri* (*SsTldE*, 3TV9), PmbA from *Pseudomonas aeruginosa* (*PaPmbA*, 3QTD), PmbA from *Bacteroides thetaiotaomicron* (*BtPmbA*, 1VPB), TldD from *T. kodakarensis* (*TkTldD*, *tk0502*), and TldD from *S. solfataricu* (*SsTldD*, *SsO0660*), revealed several conserved motifs including HExxxH, a metalloprotease-like motif, RMxNTxxxPG, and GxC in TldDs but TldEs [14] (Figure 3). The conserved residues in HExxxH and GxC motif coordinated a metal ion and was response for catalytically activity [14]. The C $^{\alpha}$ root mean square deviations between *TkTldE* and the other structural homologues *EcTldE*, *EcTldD*, 1VL4, 3TV9, 1VPB, and 3QTD were 2.6, 3.6, 2.1, 2.6, 2.5, and 2.4 Å, respectively, as determined using the DALI server (see Supplementary Materials Table S1) [25]. TldE from *T. kodakarensis* had 20–23% sequence identity and 42–53% positive matches with other TldD or TldE homologues (Table S1). Together with the fact that these proteins were found to have similar structures, this indicated that they might have similar functions.

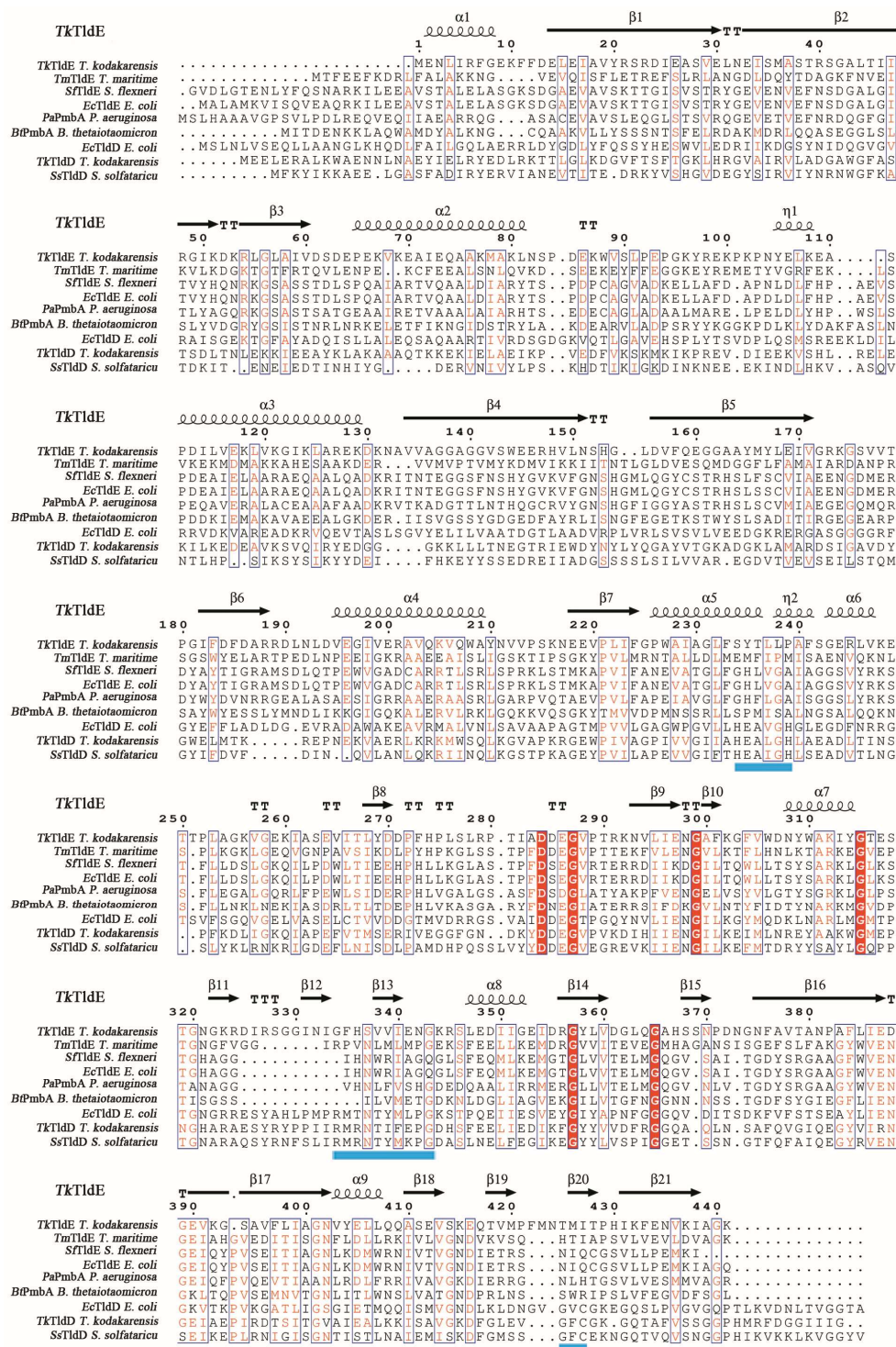


Figure 3. Structure-based amino-acid sequence alignment of *TkTldE* with other homologous proteins from different organisms: *EcTldE* (PDB: 5NJ9) and *EcTldD* (PDB: 5NJ9) from *E. coli*, *TmTldE* (PDB: 1VL4) from *T. maritime*, *SfTldE* (PDB: 3TV9) from *S. flexneri*, *PaPmbA* (PDB: 3QTD) from *P. aeruginosa*, *BtPmbA* (PDB: 1VPB) from *B. thetaiotaomicron*, *TmTldD* (Genbank accession numbers: BAD84691) from *T. kodakarensis*, and *SsTldD* (Genbank accession numbers: AAK40965) from *S. solfataricus*. Blue shaded line represented metal-binding motif (HExxxH) and conserved motifs (RMxNTxxxPG and GxC), strictly conserved residues were indicated by red shaded boxes, and similar residues were in red. The secondary structure assignment was produced using ESPrnt [26].

The function of *EcTldD*/*TldE* as a cleaving modified *MccB17* precursor in vitro was reported [14]. The structural comparison between *TkTldE* and *EcTldE*/*TldD* indicated that the overall structures were similar, but there were additional folds termed the “clamp” in *EcTldD*, which made its β -strands longer than those of *EcTldE*; this clamp was also missing in *TkTldE* and other *TldEs* (Figure 4) [14]. Cys454 coordinating a Zn^{2+} ion with two histidine residues from HExxxH motif was located in the clamp motif of *EcTldD* (Figure 4C) [15]. In contrast, Cys416 in *Sso0660*, the equivalent of Cys454 in *EcTldD* was not necessary for the metal binding but the formation of protein dimer [14]. Cysteine was not found in *TkTldE* but existed in other *TldE*/*TldDs*. Though there was a cysteine in other *TldEs* at least, cysteines were not involved in coordinating a metal ion based on structural superposition. *TkTldE* had similar folds to the “brace” motif of *EcTldD* to support the inner face of β -strands [15]. We found that two β -sheets (residues 322–333) in *TkTldE*, instead of the “brace” of *EcTldD*, supported the inner surface of six anti-parallel β -strands, but these were not found in other *TldEs* (Figure 4B). Additionally, the helix $\alpha 1$ of *TkTldE* in the N-terminal structure was shorter than that of *EcTldE*/*TldD*. Together, the reason why *TldE* cannot bind with metal ions was that the HExxxH metal-ion-binding motif was missing from *TkTldE* and *EcTldE* (Figure 3).

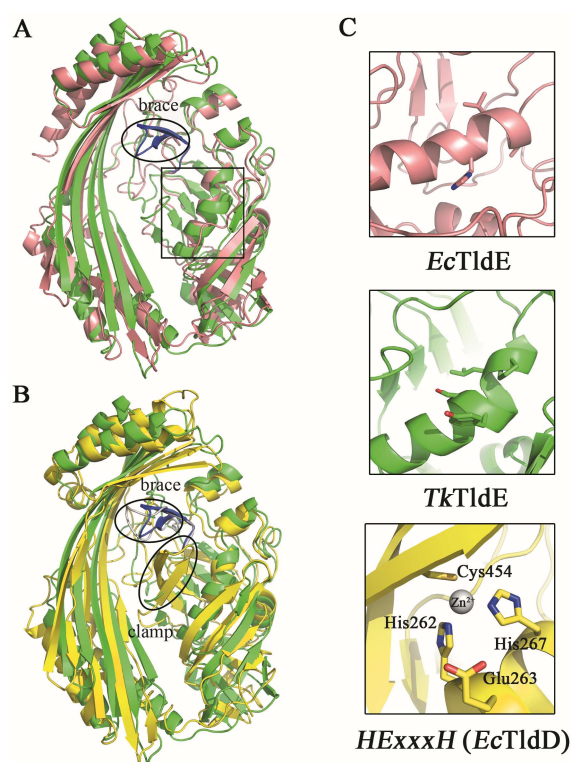


Figure 4. Structural comparison between *TkTldE* and *EcTldE*/*TldD*. (A) The ribbon diagram of *TkTldE* (green) was superimposed on that of *EcTldE* (pink). (B) Superposition of *TkTldE* and *EcTldD* (yellow). (C) Conserved residues consisting of the metal-binding motif in *EcTldD*. The metal-binding motif was shown to indicate the putative position of *EcTldD* (down), as distinguished from *TkTldE* (up) and *EcTldE* (middle). Side chains were shown as sticks.

TldD or *TldE* could form homodimers in solution, and the heterodimer of *EcTldE*/*TldD* represented an active state with the two proteins having co-evolved to directly regulate important enzymes by protein maturation or degradation [15]. The heterodimer of *EcTldE*/*TldD* was the active state, but the homodimer of *TldD* (*Sso0660*) from *S. solfataricus* was catalytically active [14,15]. We found that *tk0502* which was located next to *TldE* in the *T. kodakarensis* genome encoded a *TldD* homologue (*TkTldD*) with the HExxxH and GxC motif (Figure 3). *TkTldD* may interact with *TkTldE* to

form a heterodimer with similar function to that of *EcTldE/TldD* or form homodimer similar with *Sso0660*. Further study is needed to elucidate the connection between *TkTldE* and *TkTldD*.

In summary, the function of *TldD* and *TldE* was only investigated in the process of the maturation of *MccB17* precursor and the degradation of *CcdA* antidote. We solved the crystal structure of *TkTldE* and compared it with the structures of other homologues. Despite their overall similarity, there were distinct differences between the partial motifs of *TkTldE* and those of other *TldE/TldD* homologues. To some degree, the brace formed from two β -sheets in *TkTldE* made the structure more stable than other *TldE/TldDs*. Based on multiple sequence alignments and structural superpositions, we speculated that *TldE*, which was absent at the catalytic site in archaeal and bacterial organisms, was likely not a protease, but that it would play a functional role as a partner of metalloprotease *TldD*. The biological functions of these proteins in archaeobacteria remains to be further investigated.

Supplementary Materials: The following are available online at <http://www.mdpi.com/2073-4352/9/2/107/s1>, Figure S1: The dimer interface of *TkTldE*. Table S1: DALI statistics on structural alignment of *TkTldE* with and the other structural homologues.

Author Contributions: Conceptualization, X.Z., S.Z. and J.L.; methodology, X.Z. and Y.Z.; software, X.Z. and X.C.; validation, S.Z. and J.L.; formal analysis, X.Z., J.L.; investigation, Z.X. and Z.L.; resources, Z.L.; data curation, Y.L.; writing—original draft preparation, X.Z.; writing—review and editing, J.L.; visualization, J.L.; supervision, S.Z. and J.L.; project administration, J.L.; funding acquisition, J.L.

Funding: This research was funded by the National Key Research and Development Plan (Grant No. 2017YFD0201100).

Acknowledgments: We thank the staff of the BL-17U1 beamline at the National Facility for Protein Science Shanghai, and the Shanghai Synchrotron Radiation Facility, Shanghai, China, for assistance during data collection.

Conflicts of Interest: The authors declare no conflict of interest.

References

- Allali, N.; Afif, H.; Couturier, M.; Van Melderen, L. The Highly Conserved *TldD* and *TldE* Proteins of *Escherichia coli* are Involved in Microcin B17 Processing and in *CcdA* Degradation. *J. Bacteriol.* **2002**, *184*, 3224–3231. [[CrossRef](#)] [[PubMed](#)]
- Liu, J. Microcin B17: Posttranslational Modifications and their Biological Implications. *Proc. Natl. Acad. Sci. USA* **1994**, *91*, 4618–4620. [[CrossRef](#)]
- Rodríguez-Sáinz, M.C.; Hernández-Chico, C.; Moreno, F. Molecular Characterization of *pmbA*, an *Escherichia coli* Chromosomal Gene Required for the Production of the Antibiotic Peptide *MccB17*. *Mol. Microbiol.* **1990**, *4*, 1921–1932. [[CrossRef](#)] [[PubMed](#)]
- Genilloud, O.; Moreno, F.; Kolter, R. DNA Sequence, Products, and Transcriptional Pattern of the Genes Involved in Production of the DNA Replication Inhibitor Microcin B17. *J. Bacteriol.* **1989**, *171*, 1126–1135. [[CrossRef](#)] [[PubMed](#)]
- San Millán, J.L.; Hernández-Chico, C.; Pereda, P.; Moreno, F. Cloning and Mapping of the Genetic Determinants for Microcin B17 Production and Immunity. *J. Bacteriol.* **1985**, *163*, 275–281.
- Davagnino, J.; Herrero, M.; Furlong, D.; Moreno, F.; Kolter, R. The DNA Replication Inhibitor Microcin B17 is a Forty-Three-Amino-Acid Protein Containing Sixty Percent Glycine. *Proteins* **1986**, *1*, 230–238. [[CrossRef](#)] [[PubMed](#)]
- Li, Y.M.; Milne, J.C.; Madison, L.L.; Kolter, R.; Walsh, C.T. From Peptide Precursors to Oxazole and Thiazole-Containing Peptide Antibiotics: Microcin B17 Synthase. *Science* **1996**, *274*, 1188–1193. [[CrossRef](#)]
- Garrido, M.C.; Herrero, M.; Kolter, R.; Moreno, F. The Export of The DNA Replication Inhibitor Microcin B17 Provides Immunity for the Host Cell. *EMBO J.* **1988**, *7*, 1853–1862. [[CrossRef](#)] [[PubMed](#)]
- San Millán, J.L.; Kolter, R.; Moreno, F. Plasmid Genes Required for Microcin B17 Production. *J. Bacteriol.* **1985**, *163*, 1016–1020. [[PubMed](#)]
- Reece, R.J.; Maxwell, A. DNA Gyrase: Structure and Function. *Crit. Rev. Biochem. Mol. Biol.* **1991**, *26*, 335–375. [[CrossRef](#)]
- Herrero, M.; Moreno, F. Microcin B17 Blocks DNA Replication and Induces the SOS system in *Escherichia coli*. *Microbiology* **1986**, *132*, 393–402. [[CrossRef](#)] [[PubMed](#)]

12. Mayo, O.; Hernández-Chico, C.; Moreno, F. Microcin B17, A Novel Tool for Preparation of Maxicells: Identification of Polypeptides Encoded by the IncFII Minireplicon pMccB17. *J. Bacteriol.* **1988**, *170*, 2414–2417. [[CrossRef](#)]
13. Vizán, J.L.; Hernández-Chico, C.; del Castillo, I.; Moreno, F. The Peptide Antibiotic Microcin B17 Induces Double-Strand Cleavage of DNA Mediated by *E. coli* DNA Gyrase. *EMBO J.* **1991**, *10*, 467–476. [[CrossRef](#)] [[PubMed](#)]
14. Hu, Y.; Peng, N.; Han, W.; Mei, Y.; Chen, Z.; Feng, X.; Liang, Y.X.; She, Q. An Archaeal Protein Evolutionarily Conserved in Prokaryotes is a Zinc-Dependent Metalloprotease. *Biosci. Rep.* **2012**, *32*, 609–618. [[CrossRef](#)]
15. Ghilarov, D.; Serebryakova, M.; Stevenson, C.E.; Hearnshaw, S.J.; Volkov, D.S.; Maxwell, A.; Lawson, D.M.; Severinov, K. The Origins of Specificity in the Microcin-Processing Protease TldD/E. *Structure* **2017**, *25*, 1549–1561. [[CrossRef](#)] [[PubMed](#)]
16. Karoui, H.; Bex, F.; Dreze, P.; Couturier, M. Ham22, a Mini-F Mutation Which is Lethal to Host Cell and Promotes RecA-dependent Induction of Lambdoid Prophage. *EMBO J.* **1983**, *2*, 1863–1868. [[CrossRef](#)]
17. Maki, S.; Takiguchi, S.; Miki, T.; Horiuchi, T. Modulation of DNA Supercoiling Activity of *Escherichia coli* DNA Gyrase by F Plasmid Proteins. Antagonistic Actions of LetA (CcdA) and LetD (CcdB) Proteins. *J. Biol. Chem.* **1992**, *267*, 12244–12251.
18. Rife, C.; Schwarzenbacher, R.; McMullan, D.; Abdubek, P.; Ambing, E.; Axelrod, H.; Biorac, T.; Canaves, J.M.; Chiu, H.J.; Deacon, A.M.; et al. Crystal Structure of a Putative Modulator of DNA Gyrase (pmbA) from *Thermotoga maritima* at 1.95 Å Resolution Reveals a New Fold. *Proteins Struct. Funct. Bioinf.* **2005**, *61*, 444–448. [[CrossRef](#)]
19. Fukui, T.; Atomi, H.; Kanai, T.; Matsumi, R.; Fujiwara, S.; Imanaka, T. Complete Genome Sequence of the Hyperthermophilic Archaeon *Thermococcus kodakaraensis* KOD1 and Comparison with *Pyrococcus* Genomes. *Genome Res.* **2005**, *15*, 352–363. [[CrossRef](#)]
20. Pham, K.; LaForge, K.; Kreek, M. Sticky-end PCR: New Method for Subcloning. *Biotechniques* **1998**, *25*, 206–208.
21. Otwinowski, Z.; Minor, W. Processing of X-ray Diffraction Data Collected in Oscillation Mode. *Methods Enzymol.* **1997**, *276*, 307–326. [[PubMed](#)]
22. McCoy, A.J.; Grosse-Kunstleve, R.W.; Adams, P.D.; Winn, M.D.; Storoni, L.C.; Read, R.J. Phaser Crystallographic Software. *J. Appl. Crystallogr.* **2007**, *40*, 658–674. [[CrossRef](#)] [[PubMed](#)]
23. Emsley, P.; Cowtan, K. Coot: Model-Building Tools for Molecular Graphics. *Acta Crystallogr. D Biol. Crystallogr.* **2004**, *60*, 2126–2132. [[CrossRef](#)] [[PubMed](#)]
24. Chen, V.B.; Arendall, W.B.; Headd, J.J.; Keedy, D.A.; Immormino, R.M.; Kapral, G.J.; Murray, L.W.; Richardson, J.S.; Richardson, D.C. MolProbity: All-Atom Structure Validation for Macromolecular Crystallography. *Acta Crystallogr. D Biol. Crystallogr.* **2010**, *66*, 12–21. [[CrossRef](#)] [[PubMed](#)]
25. Holm LaRo, P. Dali Server: Conservation Mapping in 3D. *Nucleic Acids Res.* **2010**, *38*, 545–549. [[CrossRef](#)] [[PubMed](#)]
26. Robert, X.; Gouet, P. Deciphering Key Features in Protein Structures with the New ENDscript Server. *Nucleic Acids Res.* **2014**, *42*, W320–W324. [[CrossRef](#)] [[PubMed](#)]

